

Origin of anomalous surface lattice expansion in Pd(001)

S. H. Kim,^{1,*} H. L. Meyerheim,¹ J. Barthel,¹ J. Kirschner,¹ Jikeun Seo,² and J.-S. Kim³¹Max-Planck-Institut für Mikrostrukturphysik, Weinberg 2, D-06120 Halle, Germany²Department of Ophthalmic Optics, Chodang University, Muan 534-701, Korea³Department of Physics, Sook-Myung Women's University, Seoul 140-742, Korea

(Received 11 January 2005; published 27 May 2005)

We present a systematic study of the hydrogen induced anomalous expansion of the top layer spacing, d_{12} , using low-energy electron diffraction and surface x-ray scattering. After exposure of 6 L of hydrogen at 150 K sample temperature, the hydrogen atoms fully occupy the surface hollow sites and a lattice expansion of $\Delta d_{12} = +4.7\%$ is determined in agreement with theoretical predictions (5.2%). Heating the sample above the hydrogen desorption temperature ($T_D \approx 340$ K), leads to an almost complete relaxation of d_{12} to the bulk value of 1.945 Å. Similarly, no expansion is observed for clean Pd(001) prepared by rapid cooling after quick thermal treatment to remove hydrogen. Hydrogen re-adsorption from the residual gas atmosphere and possibly hydrogen agglomeration in the near surface region leads to an expansion of d_{12} in the 2%–3% range as observed in previous experiments. On the basis of our results, surface magnetism as a mechanism to trigger lattice expansion in Pd(001) does not need to be invoked.

DOI: 10.1103/PhysRevB.71.205418

PACS number(s): 68.47.De, 68.43.–h

I. INTRODUCTION

Hydrogen is well known to diffuse and dissolve efficiently in Pd, which has motivated researchers from many different disciplines to investigate the Pd–H complex due to its possible applications as hydrogen carrier.¹ Adsorption, dissociation and diffusion of hydrogen on single crystalline Pd has been studied as a model system to understand the atomistic process of hydrogen incorporation and of the catalytic behavior of Pd. For Pd(001), numerous experimental studies have been carried out by employing low-energy electron diffraction (LEED),^{2–4} He ion scattering,⁵ work function measurement,⁶ thermal desorption spectroscopy,^{6–8} nuclear reaction analysis,^{8,9} and electron energy loss spectroscopy.^{7,10} *Ab initio* calculations have been made to study the electronic and atomic structures as well as the chemical properties of Pd(001) upon hydrogen adsorption.^{11–14}

In this context, the analysis of the geometric structure of clean and hydrogen-adsorbed Pd(001) is still an unresolved problem. Behm *et al.*,² Quinn *et al.*,³ and Burchhardt *et al.*⁴ found from their LEED intensity/voltage (I/V) analysis of Pd(001) that the interlayer spacing (d_{12}) of the topmost interlayer distance is *expanded* relative to the bulk spacing ($d_B = 1.945$ Å) by $\Delta d_{12} = 2.5\%$, 3.0%, and 4.6%, respectively, while theories^{12,13,15} predict small contraction of d_{12} by -0.6% to -1.18% . An expanded top interlayer spacing is also in obvious disagreement with the general observation that the top interlayer spacing of low index metal surfaces contracts in the percent range. Such contraction is attributed to the redistribution of electrons from surface atoms to the first interlayer space.¹⁶

Two mechanisms to explain the anomalous behavior of Pd(001) were proposed by Quinn *et al.*:³ Surface magnetization and hydrogen contamination. Since bulk Pd is known to be at the verge of ferromagnetism (FM), it has often been speculated that the narrowing of the d band related to the

reduction of the coordination number at the surface could induce FM. In this picture the lattice expansion is related to the “magneto volume” effect.¹⁷ Evidence for Pd surface magnetism is not fully established yet. Magnetization of thin Pd (<5 ML) films on Ag(001)¹⁸ and Au(001)¹⁹ was investigated by magneto-optic Kerr effect, but null magnetization was found. In contrast, a recent superconducting quantum interference device investigation claimed evidence for FM at the surface of small Pd clusters.²⁰ Also theory could not give an unambiguous answer. Both self-consistent tight binding calculations²¹ and *ab initio* calculations using the full potential linearized augmented plane wave method²² predicted a delicate dependence of the magnetization on the thickness of the Pd slab which was used to model the surface structure.

On the other hand, for Pd(001) covered with hydrogen, a top layer expansion by up to 5.2% is predicted.^{11–13} This is explained by the Pd–H chemical interaction mediated by strong s - d hybridization between hydrogen and Pd-surface atoms, thereby reducing the strength of the Pd–Pd back bonding.

Despite the importance of elucidating the physical origin of the anomalous lattice expansion of Pd, no systematic experimental investigation has been carried out so far. In part this might be attributed to the fact that most classical surface analytical tools are not capable of detecting hydrogen. Furthermore, due to the ability of Pd to incorporate hydrogen into its lattice, the degree of surface contamination after preparation cycles is not well controlled and might vary from sample to sample.

The present work is aimed to systematically study the effect of hydrogen on the atomic structure of Pd(001) using LEED I/V analysis and surface x-ray diffraction (SXRD). For this purpose, Pd(001) was carefully prepared to obtain a surface as clean as possible, and exposed to hydrogen in different ways to follow previous experiments. From our study we have clear evidence that the previously reported expansion of d_{12} of “clean” Pd(001) must be attributed to

hydrogen adsorption, and that surface magnetism does not need to be invoked.

II. EXPERIMENT

LEED experiments were carried out in an UHV chamber (base pressure 5×10^{-11} mbar) equipped with a rear-view LEED optics and a cylindrical mirror analyzer for Auger electron spectroscopy. The Pd(001) sample was initially cleaned by repeated cycles of sputtering with 2 keV Ar⁺ ions followed by annealing at 950 K for 20 min. In order to remove remnant carbon, the sample was oxidized in 1×10^{-8} mbar ambient oxygen pressure at 650 K followed by a short flash to 950 K.

Before the acquisition of I/V spectra, the sample was cleaned by one cycle of sputtering followed by 30 min annealing and cooling down to room temperature (RT) which took about 60 min. In the following, this routine procedure is called the *standard* procedure. For the *standard* procedure, the total time required to complete the I/V data collection was about 2 h from the start of annealing.

It is conceivable that within the time required for setting up the experiment and to collect the data, the sample becomes contaminated by hydrogen from the residual gas atmosphere in the UHV chamber. Apart from this mechanism, an early thermal desorption study also suggested re-adsorption of hydrogen back diffused from the bulk.²³

A quantitative estimation shows that the hydrogen exposure from the residual gas atmosphere is quite small as compared to that needed for covering Pd(001) with a full monolayer (ML). Here, and in the following, we define as a ML one hydrogen atom per surface atom of Pd(001) whose areal atomic density is 1.32×10^{15} atoms/cm². Since the dominant component of the residual gas atmosphere is hydrogen, to first order it is justified to estimate the hydrogen exposure by using the total base pressure as hydrogen partial pressure. Using $p_{\text{H}_2} = 5 \times 10^{-11}$ mbar and $t = 7200$ s (2 h), the hydrogen exposure is only about 0.4 L, even if an unrealistic sticking coefficient of $s_0 = 1$ is assumed. For instance, Behm, Christman, and Ertl⁶ determined $s_0 \approx 0.5$ at 170 K and low coverage. They also found that a hydrogen exposure in the order of 5–7 L was needed to saturate the Pd(001) surface at 150 K with a monolayer (ML) of hydrogen atoms.

From this estimation, it appears reasonable to assume that in a standard experiment where the sample is first annealed and then cooled down to RT, which is slightly below the desorption temperature (T_D) of 340 K,⁷ hydrogen from the residual gas contaminates the surface within several hours, but that its coverage is well below 1 ML.

Therefore, in order to obtain a clearer picture of the hydrogen induced surface relaxation, three different types of experiments are carried out. They are focused to prepare a “really” clean surface and to prepare a surface saturated with hydrogen. Furthermore, we also try to reproduce the quite unspecific surface preparations where the surface is exposed to hydrogen by the residual gas atmosphere. In detail:

(i) In the first experiment special attention is focused to minimize hydrogen contamination from the residual gas atmosphere. This is done by cooling the crystal rapidly to 150

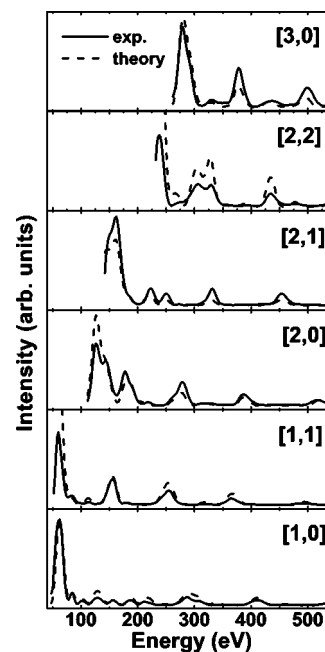


FIG. 1. LEED I/V spectra for rapidly cleaned Pd(001). Solid and dashed lines represent experimental and calculated data.

K within 30 min using liquid nitrogen. The I/V data collection is finished within 1 h after the annealing was started.

(ii) In the second experiment, I/V spectra are collected at RT after the sample is cooled down without taking extra precautions for rapid cooling (*standard* procedure). This experiment is similar to those of “clean” Pd(001) reported in the literature.^{2,3} In addition, the surface is exposed to 6 and 12 L hydrogen at RT (ambient hydrogen pressure = 1×10^{-8} mbar) and I/V spectra are collected afterwards.

For direct comparison a SXRD structure analysis is carried out for the Pd(001) also prepared by the *standard* method. For SXRD data collection, we use a z -axis diffractometer setup²⁴ and a rotating anode x-ray source in a separate UHV system. Preparation of Pd(001) follows that of the standard procedure as outlined above, except that the time required for cooling to RT and to collect a full data set equals about 40 h.

(iii) Finally, to obtain 1 ML of hydrogen covered Pd(001), we follow the preparation procedure similar to those of Ref. 6, where the sample is exposed to 6 L (at 1×10^{-8} mbar) hydrogen at 150 K. Since I/V spectra do not change for the larger hydrogen dosage, it is concluded that 6 L corresponds to 1 ML saturated coverage in agreement with the study of Behm, Christman, and Ertl.⁶

In all the experiments, a clear $p(1 \times 1)$ LEED pattern is observed for Pd(001) by visual inspection and no traces of superstructure pattern are detected.

III. STRUCTURE ANALYSIS

A. Clean Pd(001)

LEED I/V spectra are collected at normal beam incidence by a fully automated video-LEED system using a charge

TABLE I. Structure parameters for *rapidly* cleaned Pd(001). *Clean*, *Hollow H*, *Subsurface H* indicate different models used to fit the data.

	Model structure			Theory		Experiment (Quinn) ^a
	<i>Clean</i>	<i>Hollow H</i>	<i>Subsurface H</i>	LDA ^b	GGA ^c	
$\Delta d_{12}/d_B$	+0.2 ±1.4%	−0.4%	−0.4%	−0.6%	−1.0%	+3.0%
$\Delta d_{23}/d_B$	−0.7 ±1.3%	+0.0%	+0.3%		+0.1%	−1.0%
R_P factor	0.1705	0.1944	0.1941			0.350
variance	0.0206					

^aReference 3.

^bReference 12.

^cReference 13.

coupled device camera. The analysis of the recorded I/V spectra is carried out by the program SATLEED²⁵ using scattering phase shifts obtained from potentials of Moruzzi, Janak, and Williams²⁶ with l up to 10. Thermal vibration is taken into account by Debye–Waller factor with Debye temperatures of 1800 and 260 K for H and Pd, respectively.

As discussed in the following, the data are fitted using different structure models, which are tested using the Pendry R factor (R_P). Error limit of the best-fit structure is estimated by the variance of the minimum R_P factor.²⁷

In Fig. 1 the solid lines represent LEED I/V spectra for the (10), (11), (20), (21), (22), and (30) beam of the *rapidly* cleaned Pd(001) surface.²⁹ The total energy range equals 2468 eV. The dashed line corresponds to the best fit ($R_P=0.1705$) assuming clean Pd(001) with $\Delta d_{12}=+0.2(1.4)\%$ and $\Delta d_{23}=-0.7(1.3)\%$, where the numbers in brackets represent the error limit set by the variance of the minimum R_P . R_P is quite low, especially in view of the large number of beams and the wide energy range. This is also evident by direct comparison between experiment and fit, where the calculated I/V spectra (dashed lines) well reproduce the experimental ones. Different model structures were also considered, such as hydrogen in the hollow or subsurface site. Results of the I/V fit are summarized in Table I together with theoretical and experimental data reported in the literature. On the basis of R_P and its variance, the clean model is the best one. We conclude that the Pd(001) surface prepared by rapid cooling does not show any lattice expansion within the experimental accuracy. It resembles the surface structure characteristic for low index metal surfaces. In agreement with the experimental evidence, theory predicts a contraction by at most $\sim 1\%$.^{12,13,15,28}

At variance with this result, previous experiments report an expansion of 2.5–4.6%,^{2–4} possibly due to hydrogen con-

TABLE II. Structure parameters for standard preparation compared with Pd(001) dosed by 6 (6 L—H) and 12 L (12 L—H) of hydrogen at RT.

	$\Delta d_{12}/d_B$	$\Delta d_{23}/d_B$	R_P factor
<i>Standard</i>	+1.8%	−0.7%	0.1944
6 L—H	+2.4%	−0.7%	0.2095
12 L—H	+3.0%	−1.0%	0.2235

tamination. In order to test this assumption, sample preparation and I/V acquisition was carried out in a similar way as in those studies, i.e., by the standard procedure without making extra efforts to minimize the hydrogen adsorption.

B. Standard experiment

The top line on Table II lists the results of the I/V analysis. The most notable result is that d_{12} expands by 1.8%, which is in between the values found for the uncovered Pd(001) (0.2%) and previous reports (3%), supporting the speculation that expansion is related to hydrogen adsorption. However, the precise quantification of the hydrogen coverage and its relation to Δd_{12} is not straightforward, since the detailed conditions might vary from experiment to experiment. We roughly estimate an upper limit of the hydrogen exposure in the standard experiment as follows: assuming a sticking coefficient of $s_0=1$, the surface is exposed only to about 0.4 L hydrogen during 2 h with $p_{H_2}=5 \times 10^{-11}$ mbar. This number has to be compared with studies where a calibration of the hydrogen coverage was carried out: At 110 K, the hydrogen coverage saturates with the 2–4 L of dosage.³⁷ At 170 K, Behm, Christman, and Ertl⁶ report—albeit indirectly on the basis of the work function change—that an exposure of about 6 L is needed to deposit 1 ML of hydrogen on the Pd(001) surface. In a later TD study by Okuyama,⁷ the β peak related to fourfold-hollow adsorption is near saturation already after 2.4 L exposure at 200 K.

In summary, all these studies indicate that an exposure at least one order of magnitude larger than estimated is needed to saturate the Pd(001) surface with 1 ML of hydrogen. On the other hand, theory suggests a lattice expansion of 5.2% for 1 ML of hydrogen on Pd(001).^{11–13} Therefore it can be concluded that the estimated upper limit of the exposure (0.4 L) and the experimentally determined lattice expansion (1.8%) do not fit on a linear scale to the exposure needed for 1 ML (6 L) and the calculated expansion (5.2%).

Another complication, which makes the quantification of the (near) surface hydrogen coverage difficult, arises from the fact that hydrogen dissolved in the bulk might diffuse to the near surface regime. This has already been noted in an early paper by Conrad, Ertl, and Latta²³ on the adsorption of hydrogen on Pd(110) and Pd(111). Similarly, for Pd(001), Okuyama *et al.*⁷ observe a TD peak in the 300 K range,

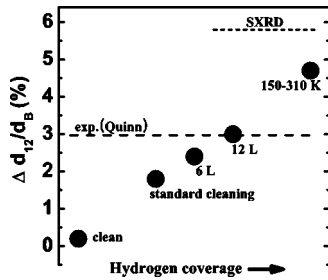


FIG. 2. $\Delta d_{12}/d_B$ vs hydrogen coverage. The abscissa is not to scale. Filled circles labeled by clean, standard cleaning, 6 L, 12 L, and 150–310 K refer to LEED I/V experiments. The dotted and dashed line correspond to the lattice expansions derived from the SXR data and the LEED analysis of Quinn *et al.* (see Ref. 3), respectively.

which is also attributed to subsurface hydrogen.

While the clarification of how the lattice expansion scales with the hydrogen coverage also be the subject of theoretical work, from the experimental view it appears tempting to test the exposure versus Δd_{12} dependence by dosing different amounts of hydrogen and to analyze the surface structure.

The second and third line of Table II list the structure parameters obtained after deposition of 6 and 12 L hydrogen deposited at RT. It is to note that only d_{12} and d_{23} are considered, while the position of the hydrogen atoms was not refined. We have also carried out I/V analysis using the average t -matrix approximation³⁰ where the composition of the surface hydrogen is treated as an additional fitting parameter. We find that both d_{12} and d_{23} are not very sensitive to whether or not hydrogen is included in the structure model. In contrast, there is large uncertainty in the hydrogen coverage and position due to its small scattering cross section. In Table II, we find $\Delta d_{12}=2.4\%$ and 3.0% . The data can be interpreted that there is some dependence of d_{12} on the hydrogen coverage. When 12 L of hydrogen are dosed, Δd_{12} is $+3\%$, which is approximately equivalent to Quinn's result obtained for their clean sample.

This is also schematically shown in Fig. 2, where $\Delta d_{12}/d_B$ (solid circles) is plotted versus the hydrogen coverage and the dashed line represents Quinn's result. Note that the abscissa is not to scale.

An independent analysis of the lattice relaxation using a different Pd crystal was carried out by SXR. While SXR is in general less sensitive to vertical structure parameters than LEED, its advantage lies in the applicability of the single scattering theory. In many cases this provides an easier and more direct analysis of the data as compared to LEED as will be discussed in the following:

For the SXR data collection, x rays were generated by a rotating anode system. Emitted x rays (Cu $K\alpha$ radiation) are monochromatized and focused onto the sample by using a multilayer optics yielding a peak count rate of several hundred counts per second at the anti-phase conditions along the crystal truncation rods (CTRs).^{31,32} Integrated x-ray reflection intensities were collected under total reflection conditions of the incoming beam (incidence angle $\alpha_i \approx 0.32^\circ$) by rotating the sample around its surface normal.^{31,32} In this way the intensity distribution along the (10), (20), (11), and

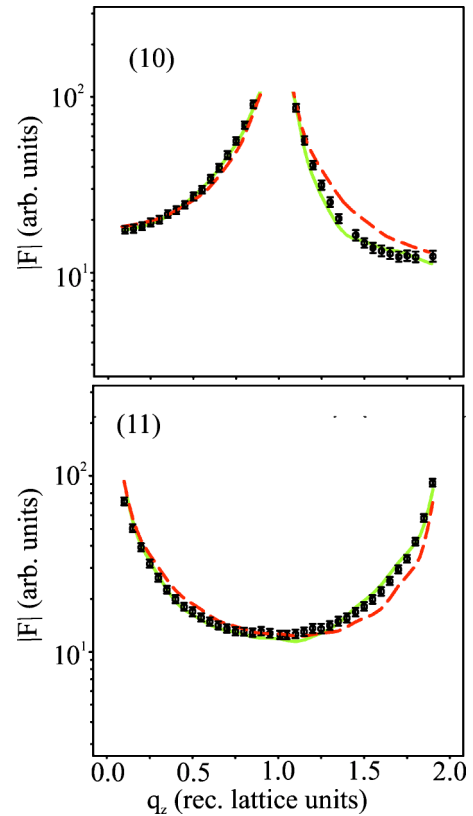


FIG. 3. (Color online) Experimental (symbols) and calculated (lines) structure factor amplitudes along the (10) and the (11) CTR. Continuous green line corresponds to $|F|$ calculated for Pd(001) with $\Delta d_{12}=+5.8\%$. Dashed red line is for bulk-terminated Pd(001).

(21) CTRs was collected up to a maximum momentum transfer normal to the sample surface ($q_z=2.90 \text{ \AA}^{-1}$, corresponding to 1.8 reciprocal lattice units (rlu)). Symbols in Fig. 3 represent the experimental structure factor amplitudes, $|F|$, along the (10) and the (11) CTR after correcting the integrated intensities for geometric factors.³³

For bulk truncated crystals, the intensity distribution along CTR's has a characteristic U-shape, which is symmetric around the anti-phase condition³². Any relaxation of the interlayer spacing induces a deviation of this symmetry. Expansion (contraction) of d_{12} leads to a shift of the CTR minimum to lower (larger) q_z . In Fig. 3 this is shown by the dashed and solid line, which correspond to $|F|$'s calculated for bulk truncated Pd(001) and for $\Delta d_{12}=5.8\%$, respectively. Even by direct inspection it is evident that the solid lines better fit the data, corresponding to expanded d_{12} . Structure parameters were refined by least square fitting of the data including all four CTRs corresponding to 136 symmetry independent reflections.³⁴ Apart from an overall scale factor, the first two interlayer distances, d_{12} , d_{23} and the Debye parameters (B) of the top four Pd layers were varied. The De-

TABLE III. Results of the SXR analysis.

$\Delta d_{12}/d_B$	$\Delta d_{23}/d_B$	$B_1 [\text{\AA}^2]$	$B_2 [\text{\AA}^2]$	$B_3 [\text{\AA}^2]$	$B_4 [\text{\AA}^2]$
$+5.8(2.6)\%$	$2.4(2.8)\%$	$2.6(0.3)$	$2.6(0.3)$	$2.1(0.2)$	$1.7(0.2)$

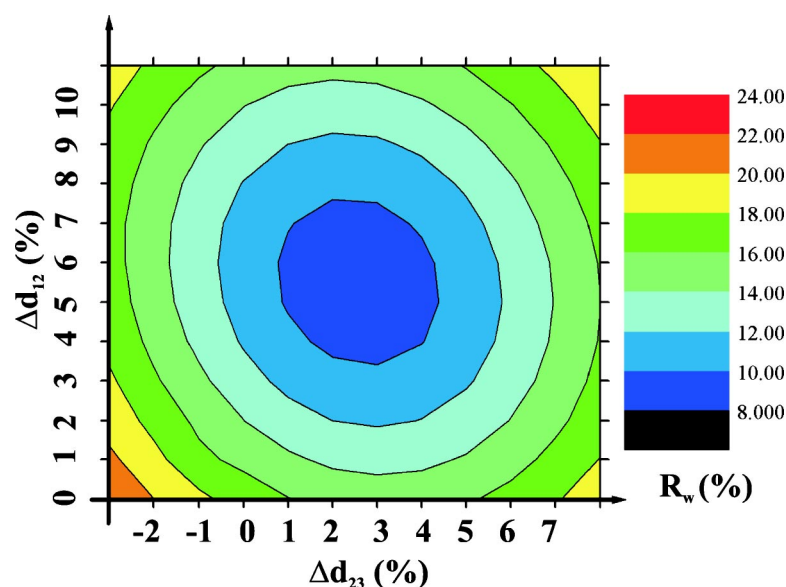


FIG. 4. (Color online) Contour plot of R_w vs Δd_{12} and Δd_{23} .

bye parameter is related to the mean square displacement amplitude, $\langle u^2 \rangle$, according to the relation: $B = 8 \times \pi^2 \langle u^2 \rangle$. The B 's of the deeper layers were kept constant at the bulk value ($B = 0.4 \text{ \AA}^2$) corresponding to the Debye temperature of 260 K.³⁵

No attempt was made to include hydrogen into the refinement, since x-ray diffraction is much less sensitive to weak scatterers than LEED in general. A summary of the fit results is presented in Table III. Error bars as derived from the variance-covariance matrix are given in brackets.

The most important result is the significant expansion of d_{12} by $5.8 \pm 2.6\%$. This is represented by the dotted line in Fig. 2. Furthermore, the SXR data also indicate a second layer expansion ($\Delta d_{23} = 2.4 \pm 2.8\%$), although the error bar is large in this case. There is a pronounced dependence of weighted residual, R_w , on the interlayer spacing. Figure 4 shows a contour plot of the weighted residual, R_w ³⁶ vs Δd_{12} and Δd_{23} . For the bulk truncated crystal, R_w is in the 18% range, while for the best fit R_w equals 8.9%.

In summary, the SXR data indicate a considerably larger interlayer spacing as compared to the LEED analysis of the "standard" samples, for which Δd_{12} values between 1.8% (this work) and about 3%³ are found. It is rather comparable

to that predicted theoretically for 1 ML hydrogen coverage (5.2%).¹² A rough estimation of the hydrogen coverage for this particular experiment shows that the comparatively large expansion could be related to a correspondingly larger hydrogen coverage. Considering the much longer time needed, e.g., to cool down the sample, to measure a sufficiently redundant data set (in the order of 40 h in total) and the higher hydrogen pressure in the SXR chamber ($\approx 10^{-10}$ mbar), the exposure of Pd(001) to residual hydrogen during SXR measurement is in the range needed for saturation coverage of the surface (≥ 10 L) even after a fraction of the total experimental time. Furthermore, based on the expansion of d_{23} and the enhanced Debye parameters for the top layers, it is tempting to speculate that in the present case subsurface hydrogen could also play a role.

C. 1 ML H on Pd(001)

In contrast to the poorly quantified hydrogen coverages for samples prepared by the standard method, it is known that exposure of about 6 L at 170 K leads to a Pd(001) covered by about 1 ML hydrogen.⁶ After preparing the sample using this recipe, I/V spectra were collected and ana-

TABLE IV. Structure parameter for 1 ML H on Pd(001) at 150 K. Distances d_H and d_{12} are defined in Fig. 6. Other model structures and the related R_p factors are shown for comparison.

	Model structure				Theory		
	Hollow H	Bridge H	On-top H	Clean	LDA ^b	GGA ^c	Experiment ^a
d_H	$0.20^{+0.43}_{-0.22} \text{ \AA}$	1.21 \AA	1.10 \AA		0.16 \AA (Hollow)	0.20 \AA	0.3 \AA
$\Delta d_{12}/d_b$	$+4.7 \pm 1.1\%$	+5.2%	+5.8%	+5.3%	+5.2%	+4.4%	$(d_H + \Delta d_{12})$
$\Delta d_{23}/d_b$	$+0.0 \pm 0.9\%$	-1.0%	-0.1%	-0.4%		0.2%	
R factor	0.1626	0.2720	0.3594	0.2646			
variance	0.0231						

^aReference 9.

^bReference 12.

^cReference 13.

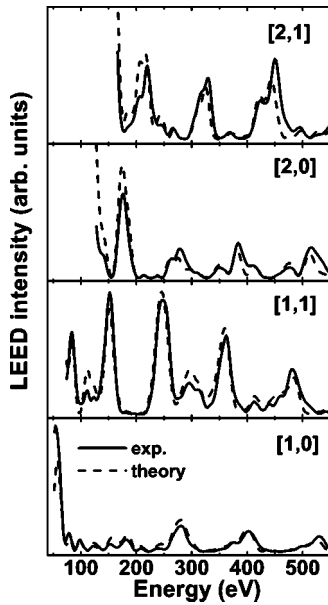


FIG. 5. LEED I/V spectra for Pd(001) exposed to 6 L hydrogen at 150 K. Solid and dashed lines represent experimental and calculated I/V spectra.

lyzed. In addition, data collection was carried out after heating the sample to different temperatures between 220 and 430 K. At 340 K, hydrogen is known to desorb from the Pd(001) surface,⁷ which is expected to have a notable effect on the top layer spacings.

Table IV provides a summary of the results. First we discuss the atomic structure of hydrogen-adsorbed Pd(001) at 150 K. I/V spectra were collected for the (10), (11), (20), and (21) beams as shown in Fig. 5. The best fit is obtained for a model where 1 ML of hydrogen is adsorbed in the fourfold hollow site of Pd(001) (Fig. 6). We find that the theoretical I/V spectra for the best-fit structure reproduce all the experimental features. The R_p factor of the best-fit structure is notably low (0.1626) and the R_p factors derived for the other models are by far outside the variance of the minimum R_p .

The hydrogen adsorption height (d_H) equals 0.2 Å. The top layer spacing d_{12} expands by 4.7%, while d_{23} and d_{34} show no relaxation within the error limits. These values are in excellent agreement with recent theoretical predictions

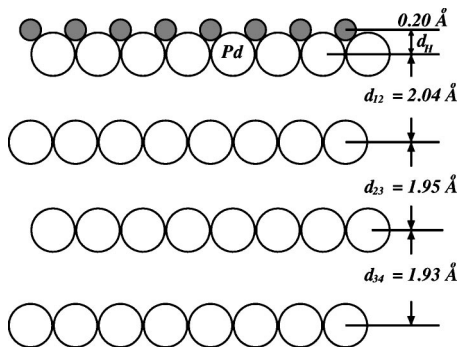


FIG. 6. Schematic structure model for 1 ML hydrogen on Pd(001) as derived from the analysis of the I/V spectra shown in Fig. 5.

TABLE V. Structure parameters derived from LEED I/V data for Pd(001) exposed to 6 L hydrogen at 150 K followed by heating to temperatures as indicated.

Exp. temp.	Hollow H			Clean	
	d_H	$\Delta d_{12}/d_B$	R_p factor	$\Delta d_{12}/d_B$	R_p factor
220 K	0.20 Å	+4.5%	0.1692	+5.3%	0.2582
250 K	0.20 Å	+4.4%	0.1748	+5.2%	0.2658
280 K	0.21 Å	+4.4%	0.1826	+5.2%	0.2733
310 K	0.21 Å	+4.2%	0.2088	+5.1%	0.2931
340 K	0.44 Å	+0.5%	0.2007	+0.9%	0.2004
400 K	0.33 Å	+0.6%	0.1956	+0.6%	0.1873
430 K	0.61 Å	+0.7%	0.2043	+0.8%	0.1899

that the fourfold hollow site is the energetically most favored adsorption site.¹²

In the next step, the evolution of the lattice relaxation during sample heating up to temperatures higher than the desorption temperature, T_D , was analyzed. Hydrogen desorption is expected to result in a corresponding relaxation of d_{12} from expanded to almost bulklike. The results of the LEED I/V analysis (see Table V) confirm this expectation. Structure parameters, d_H and d_{12} , for both model structures, 1 ML of hydrogen adsorbed in the hollow sites and clean Pd(001), are listed as a function of sample temperature together with their corresponding R_p factors. Between 310 and 340 K there is a significant change, where the best-fit model switches from 1 ML hydrogen adsorbed structure to clean Pd(001). Simultaneously, the expansion of d_{12} nearly vanishes, and d_{23} also develops small structural change near the same temperature range, as summarized in Fig. 7. This picture is consistent with the model that in the temperature regime between 310 and 340 K hydrogen desorbs from the surface.^{7,8}

IV. SUMMARY

We have systematically investigated hydrogen-induced surface relaxation of Pd(001). We find a top layer expansion

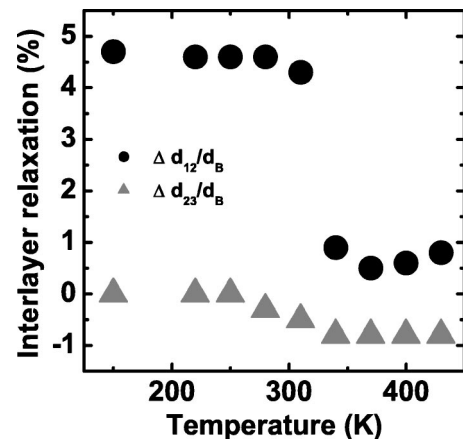


FIG. 7. Dependence of Δd_{12} and Δd_{23} on sample temperature.

of $\Delta d_{12}=4.7\%$ for 1 ML of hydrogen-covered Pd(001) that is formed by exposing the sample to 6 L at 150 K. This is in reasonable agreement with theoretical predictions (5.2%). In contrast, the clean Pd(001), prepared either by desorption of the as-deposited hydrogen or by rapid cooling after flashing does not show any evidence for top layer expansion within our experimental accuracy. This corresponds to general observations on low index metal surfaces.

Furthermore, experiments intended to reproduce previous studies on the structure of clean Pd(001) indicate that after the cleaning procedure the surface becomes rapidly contaminated by hydrogen, inducing a top layer expansion in the range of 2%–3%. A rough estimation of the hydrogen expo-

sure in these cases leads to the conclusion that there is no simple linear relation between hydrogen coverage and inter-layer spacing.

In view of our study, it is not necessary to invoke surface magnetism as a mechanism to trigger lattice expansion in Pd(001).

ACKNOWLEDGMENTS

The authors thank G. Kroder for technical support during the experiments. This work is partly supported by KOSEF through CSCMR (J.K.).

*Present address: Department of Ophthalmic Optics, Kwangju Health College, Kwangju, Korea.

¹*Metal Hydrides*, edited by W. M. Mueller, J. P. Blackledge, and G. G. Libowitz (Academic Press, New York, 1986).

²R. J. Behm, K. Christman, G. Ertl, M. A. Van Hove, P. A. Thiel, and W. H. Weinberg, *Surf. Sci.* **88**, L59 (1979).

³J. Quinn, Y. S. Li, D. Tian, H. Li, and F. Jona, *Phys. Rev. B* **42**, 11 348 (1990).

⁴J. Burchhardt, E. Ludgren, M. M. Nielsen, J. N. Andersen, and D. L. Adams, *Surf. Rev. Lett.* **3**, 1339 (1996).

⁵K. H. Rieder and W. Stocker, *Surf. Sci.* **148**, 139 (1984).

⁶R. J. Behm, K. Christman, and G. Ertl, *Surf. Sci.* **99**, 320 (1980).

⁷H. Okuyama, W. Siga, T. Takagi, M. Nishijima, and T. Aruga, *Surf. Sci.* **401**, 344 (1998).

⁸M. Wilde, M. Matsumoto, K. Fukutani, and T. Aruga, *Surf. Sci.* **482–485**, 346 (2001).

⁹F. Besenbacher, I. Stensgaard, and K. Mortensen, *Surf. Sci.* **191**, 288 (1987).

¹⁰C. Nyberg and C. G. Tengstøl, *Phys. Rev. Lett.* **50**, 1680 (1983).

¹¹D. Tománek, Z. Sun, and S. G. Louie, *Phys. Rev. B* **43**, 4699 (1991).

¹²S. Wilke, D. Hennig, and R. Löber, *Phys. Rev. B* **50**, 2548 (1994).

¹³A. Eichler, J. Hafner, and G. Kresse, *J. Phys.: Condens. Matter* **8**, 7659 (1996).

¹⁴S. Wilke and M. Scheffler, *Phys. Rev. B* **53**, 4926 (1996).

¹⁵I. G. Batirev, *Philos. Mag. Lett.* **73**, 385 (1996).

¹⁶P. J. Feibelman, *Surf. Sci.* **360**, 297 (1996).

¹⁷V. L. Moruzzi and P. M. Marcus, *Phys. Rev. B* **39**, 471 (1989).

¹⁸R. L. Fink, C. A. Ballentine, J. L. Erskine, and J. Araya-Pochet, *Phys. Rev. B* **41**, 10 175 (1990).

¹⁹C. Liu and S. D. Bader, *Phys. Rev. B* **44**, 12 062 (1991).

²⁰B. Sampedro, P. Crespo, A. Hernando, R. Litrán, J. C. Sánchez López, C. López Cartes, A. Fernandez, J. Ramirez, J. González Calbet, and M. Vallet, *Phys. Rev. Lett.* **91**, 237203 (2003).

²¹H. Dreyssé, A. Mokrani, S. Bouarab, and C. Demangeat, *Surf. Sci.* **251–252**, 41 (1991).

²²S. C. Hong (unpublished).

²³H. Conrad, G. Ertl, and E. E. Latta, *Surf. Sci.* **41**, 435 (1974).

²⁴M. Bloch, *J. Appl. Crystallogr.* **18**, 33 (1985).

²⁵P. J. Rous, J. B. Pendry, D. K. Saldin, K. Heinz, K. Müller, and N. Bickel, *Phys. Rev. Lett.* **57**, 2951 (1986); A. Wander, M. A. van Hove, and G. A. Somorjai, *ibid.* **67**, 626 (1991).

²⁶V. L. Moruzzi, J. F. Janak, and A. R. Williams, *Calculations of Electronic Properties of Metals* (Pergamon, New York, 1978).

²⁷J. B. Pendry, *J. Phys. C* **13**, 937 (1980).

²⁸M. Methfessel, D. Henig, and M. Scheffler, *Phys. Rev. B* **46**, 4816 (1992).

²⁹We use a sample setting corresponding to a primitive surface unit cell, where the surface (*s*) setting is related to the face centered cubic setting of the bulk (*b*) by the following relations: $[100]_s = 1/2 \times ([100]_b - [010]_b)$; $[010]_s = 1/2 \times ([100]_b + [010]_b)$ and $[001]_s = [001]_b$.

³⁰F. Jona, K. O. Legg, H. D. Shih, D. W. Jepsen, and P. M. Marcus, *Phys. Rev. Lett.* **40**, 1466 (1978); Y. Gauthier, Y. Joly, R. Baudouin, and J. Rundgren, *Phys. Rev. B* **31**, 6216 (1985).

³¹R. Feidenhans'l, *Surf. Sci. Rep.* **10**, 105 (1989).

³²I. K. Robinson and D. J. Tweet, *Rep. Prog. Phys.* **55**, 599 (1992).

³³E. Vlieg, *J. Appl. Crystallogr.* **30**, 532 (1997).

³⁴Derived from 194 reflections after averaging over symmetry equivalent reflections. Standard deviations were obtained from the weighted sum of the average agreement factor between symmetry equivalent reflections (7.6%) and the statistical errors.

³⁵*International Tables for Crystallography*, edited by A. Wilson (Kluwer, Dordrecht, 1985), Vol. C.

³⁶The weighted residual R_w is defined by $R_w = \sqrt{\frac{\sum w(|F_{\text{obs}}| - |F_{\text{calc}}|)^2}{\sum w|F_{\text{obs}}|^2}}$, where F_{obs} and F_{calc} are the observed and calculated structure factors, respectively, and $w = 1/\sigma^2$ is weighting factor using the standard deviation (σ) as parameter. The summation runs over all data points.

³⁷M. L. Burke and R. J. Madix, *Surf. Sci.* **237**, 1 (1990).